Synthesis, Swelling Behaviors, and Slow-Release Characteristics of a Guar Gum-*g*-Poly(sodium acrylate)/Sodium Humate Superabsorbent

Wenbo Wang,[1,2] Aiqin Wang[1]

[1]*Center of Eco-Materials and Green Chemistry, Lanzhou Institute of Chemical Physics, Chinese Academy of Sciences, Lanzhou 730000, People's Republic of China*
[2]*Graduate University of the Chinese Academy of Sciences, Beijing 100049, People's Republic of China*

Received 8 June 2008; accepted 1 November 2008
DOI 10.1002/app.29620
Published online 13 February 2009 in Wiley InterScience (www.interscience.wiley.com).

ABSTRACT: Superabsorbents used in agricultural and ecological projects with low-cost, slow-release fertilizers and environmentally friendly characteristics have been extensively studied. The use of a natural polymer as the matrix and then further polymerization with some functional material has become the preferred method. In this work, with natural guar gum (GG), partially neutralized acrylic acid, and sodium humate (SH) as the raw materials, ammonium persulfate as the initiator, and *N*,*N*′-methylenebisacrylamide (MBA) as the crosslinker, GG-*g*-poly(sodium acrylate) (PNaA)/SH superabsorbents were synthesized through a solution polymerization reaction and were characterized with Fourier transform infrared spectroscopy, scanning electron microscopy, and thermogravimetric analysis. The effects of the SH content and MBA concentration on the water absorbency were investigated. The results showed that the introduction of SH into the GG-*g*-PNaA system could improve the water absorbency, swelling rate, pH-resistant property, and reswelling capability, and the superabsorbent containing 15 wt % SH had the highest water absorbency of 532 g/g of sample in distilled water and 62 g/g of sample in a 0.9 wt % NaCl solution. The slow release in water and water retention in sandy soil tests revealed that the superabsorbent could act as a fertilizer as well as an effective water-saving material for agricultural applications. © 2009 Wiley Periodicals, Inc. J Appl Polym Sci 112: 2102–2111, 2009

Key words: graft copolymers; high performance polymers; hydrophilic polymers; swelling; synthesis

INTRODUCTION

Superabsorbents can absorb and retain huge volumes of aqueous fluids even under some pressure in comparison with traditional water-absorbing materials and have exhibited potential applications in many fields such as hygienic products,[1] drug-release carriers,[2] and wastewater treatment.[3,4] As water-manageable materials, superabsorbents have shown some encouraging effects in modern agriculture and have exhibited great potential and perspective.[5–7] However, there are limitations to such applications because the superabsorbents used in practice are expensive synthetic polymers that are simple in function, not suitable for salt-containing soils, and poor with respect to biodegradability.[8] Currently, the design and synthesis of novel agricultural superabsorbents is a significant subject.

It is well known that the growth of plants and their quality are affected not only by water but also by fertilizer; synchronous improvement of the utilization of water resources and fertilizer nutrients is expected. As is known, the most effective method of reducing fertilizer losses involves the use of slow- or controlled-release fertilizers.[9] Therefore, further research related to agricultural superabsorbents has been directed toward slow-release superabsorbents with environmentally friendly characteristics. Recently, the use of low-cost, annually renewable, and biodegradable natural polysaccharides and substitutes for petroleum-based polymers has shown commercial and environmental advantages.[10] The use of a natural polymer as the matrix and then polymerization with other low-cost functional materials has become the preferred method to achieve performances expected to be superior to those of the matrix materials and to improve environmentally friendly properties. To the best of our knowledge, natural macromolecules such as starch,[11,12] cellulose,[13,14] chitosan,[15,16] alginate,[17] and carrageenan[18]

Correspondence to: A. Wang (aqwang@lzb.ac.cn).
Contract grant sponsor: West Light Foundation and Western Action Project of the Chinese Academy of Sciences; contract grant number: KGCX2-YW-501.
Contract grant sponsor: 863 Project of the Ministry of Science and Technology, People's Republic of China; contract grant numbers: 2006AA03Z0454 and 2006AA100215.

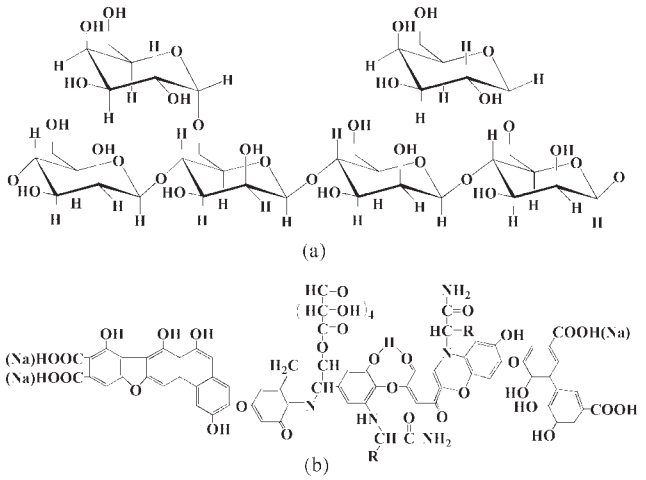

Scheme 1 Chemical structures of (a) GG and (b) SH.

and their derivatives have been investigated. However, there is little literature focused on superabsorbents based on natural vegetable gums with unique structures and special properties.

Guar gum (GG), a representative natural vegetable gum, is a branched polymer with β-D-mannopyranosyl units linked (1–4) with single-member α-D-galactopyranosyl units occurring as side branches [Scheme 1(a)]. GG and its derivatives have been used in different applications, such as thickeners, ion-exchange resins, and suspending agents.[19] As a matrix polymer for preparing a superabsorbent, GG through its nonionic side arms is expected to improve the water-absorption and salt-resistant properties of the resulting superabsorbent. Sodium humate (SH) is composed of multifunctional aliphatic and aromatic components and contains large numbers of functional hydrophilic groups such as carboxylates and phenolic hydroxyls [Scheme 1(b)]. SH can regulate plant growth, accelerate root development, improve soil cluster structures, and improve the absorption of nutrient elements. It has been introduced into poly(acrylate) and poly(acrylic acid-*co*-acrylamide) networks by our group.[20–22] On the basis of our previous work about a superabsorbent containing SH, in this study, GG-*g*-poly(sodium acrylate) (PNaA)/SH superabsorbents were synthesized through a solution polymerization reaction. The effects of the SH content and *N*,*N*′-methylenebisacrylamide (MBA) concentration on the water absorbency were investigated. The swelling rate, pH-resistant property, reswelling capability, and slow-release characteristics were also evaluated.

EXPERIMENTAL

Materials

GG (food-grade; number-average molecular weight = 220,000) was from Wuhan Tianyuan Biology Co. (Wuhan, China). Acrylic acid (AA; chemically pure; Shanghai Wulian Chemical Factory, Shanghai, China) was distilled under reduced pressure before use. Ammonium persulfate (analytical-grade; Xi'an Chemical Reagent Factory, Xi'an, China) was recrystallized before use. MBA (chemically pure; Shanghai Chemical Reagent Corp., Shanghai, China) was used as purchased. SH micropowder (Shuanglong, Ltd., Xinjiang, China) was milled and passed through a 320-mesh screen before use. The sandy soil used for water-retention testing was taken from the Tenggeli Desert (Inner Mongolia, China).

Preparation of the GG-*g*-PNaA/SH and GG-*g*-PNaA superabsorbents

GG (1.20 g) was dispersed in 34 mL of an NaOH solution (pH = 12.5, 0.067 mol/L) in a 250-mL four-necked flask equipped with a mechanical stirrer, a reflux condenser, a thermometer, and a nitrogen line. Under a nitrogen atmosphere, the obtained dispersive solution was heated to 60°C in an oil bath for 1 h to form a colloidal slurry. An aqueous solution (4 mL) of the initiator ammonium persulfate (0.0864 g) was then added to the slurry, and the resulting mixture was stirred for 10 min to generate radicals. AA (7.2 g) was neutralized with 8.5 mL of 8 mol/L NaOH to reach a total neutralization degree of 70% (34 mL of a 0.067 mol/L NaOH solution, used to disperse GG, was also calculated as part of the neutralization degree), and then 10 mg of the crosslinker MBA and 1.51 g of SH micropowder were added to the neutralized AA solution under magnetic stirring, forming a uniform mixture solution. After the reactants were cooled to 40°C, the mixture solution was added to the reaction flask. Then, the oil bath was slowly heated to 70°C and kept there for 3 h. A nitrogen atmosphere was maintained throughout the reaction period. The obtained gel products were dried in an oven at 70°C to a constant weight; the dried samples were ground and had a particle size of 40–80 mesh (180–380 μm).

The GG-*g*-PNaA superabsorbent hydrogel was prepared according to a similar procedure but without SH.

Measurements of the water absorbency and swelling kinetics in distilled water

A 0.05-g sample was immersed in excessive aqueous liquids for 4 h to reach swelling equilibrium. The swollen gels were filtered out with a mesh screen and then drained on the sieve for 10 min. After the swollen samples were weighed, the equilibrium water absorbency of the superabsorbent was calculated with eq. (1):

$$Q_{eq} = (w_s - w_d)/w_d \quad (1)$$

where Q_{eq} is the equilibrium water absorbency (g/g of sample), which is an average of three measurements, and w_d and w_s are the weights of the dry sample and swollen sample, respectively.

The swelling kinetics of the superabsorbents were measured as follows. An accurate amount of each sample (0.05 g) was immersed in excess distilled water. The swollen sample was then filtered out with a mesh screen and weighed at set intervals. This procedure was repeated until the weight of the swollen sample remained constant. The water absorbency at any given moment could be calculated according to eq. (1).

Measurement of the water absorbency in various pH solutions

The pH of external solutions was adjusted with standard 1 mol/L HCl or NaOH aqueous solutions. The method of determining the water absorbency in solutions of various pHs was similar to that used in distilled water, and the volume of the solution used for determining water absorbency was chosen to be 200 mL. After the swollen gels were filtered out, the pH of the filtrate was also measured with a pH meter (320 pH meter, Mettler–Toledo, Zurich, Switzerland) to evaluate the change in the pH resulting from the swelling of the superabsorbents.

Measurement of the slow-release behaviors

Accurately weighed samples (0.30 g) were soaked in 500 mL of distilled water in a beaker at room temperature. Exactly 5.00 mL of the solution was transferred from the beaker into a 10-mL test tube at each fixed time interval. The test solution was oxidized at 100°C by the addition of 3.0 mL of a $K_2Cr_2O_7$ solution [$C(1/6K_2Cr_2O_7) = 0.8$ mol/L] and 15 mL of concentrated H_2SO_4 [eq. (2)]. The residual $K_2Cr_2O_7$ was titrated with an $(NH_4)_2Fe(SO_4)_2$ solution [0.1 mol/L; eq. (3)]. The release of SH was expressed with the carbon content [C (mg/5 mL)] in the solution [eq. (4)]:

$$2K_2Cr_2O_7 + 3C + 8H_2SO_4 \rightarrow 2K_2SO_4 + 2Cr_2(SO_4)_3 + 3CO_2 + 8H_2O \quad (2)$$

$$K_2Cr_2O_7 + 7H_2SO_4 + 6FeSO_4 \rightarrow K_2SO_4 + Cr_2(SO_4)_3 + 3Fe_2(SO_4)_3 + 7H_2O \quad (3)$$

$$C(\text{mg}/5\text{ mL}) = 12.01C_{Fe}^{2+}(V_0 - V_1)/4 \quad (4)$$

where C_{Fe}^{2+} is the concentration of the $(NH_4)_2Fe(SO_4)_2$ solution (mol/L); V_0 is the volume of the $(NH_4)_2Fe(SO_4)_2$ solution used to titrate residual $K_2Cr_2O_7$ in the blank solution, that is, lixivium of GG-*g*-PNaA (mL); V_1 is the volume of the $(NH_4)_2Fe(SO_4)_2$ solution used to titrate the residual $K_2Cr_2O_7$ in the test solution (mL); 12.01 is the molar weight of carbon (g/mol); and the constant 4 is the molar ratio of Fe^{2+} to carbon according to eqs. (2) and (3).

Measurement of the water-retention properties in sandy soil

A sample of GG-*g*-PNaA/SH (15 wt %; 0.2, 0.5, 1.0, or 2.0 g) was well mixed with 200 g of dry sandy soil and kept in ventilated paper cups. Then, 100 mL of tap water was slowly added to these cups and weighed (w_1). A controlled experiment without the superabsorbent was also carried out. The cups were maintained at 25°C (relative air humidity = 28%) and were weighed at a certain interval (w_i). The water retention ratio [w (%)] of sandy soil was calculated with eq. (5):

$$w(\%) = 1 - (w_1 - w_i)/100 \quad (5)$$

Reswelling capability

The sample (0.05 g) was soaked in 100 mL of distilled water to achieve the swelling equilibrium, and then the swollen sample was placed in an oven to dehydrate at 100°C. After thorough drying, an equal volume of water was added to the recovered superabsorbent to reach the swelling equilibrium. The swollen samples were dehydrated by the aforementioned procedure again. A similar procedure was repeated several times to evaluate the reswelling capabilities of the superabsorbents.

Characterization

The Fourier transform infrared (FTIR) spectra were recorded on a Nicolet Nexus FTIR spectrometer (Madison, WI) in the 4000–400 cm^{-1} region with KBr pellets. The thermal stability of the samples was studied on a PerkinElmer TGA-7 thermogravimetric analyzer (PerkinElmer Cetus Instruments, Norwalk, CT) with a temperature range of 25–800°C at a heating rate of 10°C/min with a dry nitrogen purge at a flow rate of 50 mL/min. The morphologies of the samples were examined with a JSM-6701F field emission scanning electron microscope (JEOL, Tokyo, Japan) after the samples were coated with a gold film.

RESULTS AND DISCUSSION

FTIR spectra

The FTIR spectra of SH, GG, a physical mixture of GG and PNaA (weight ratio of PNaA to GG = 6.0),

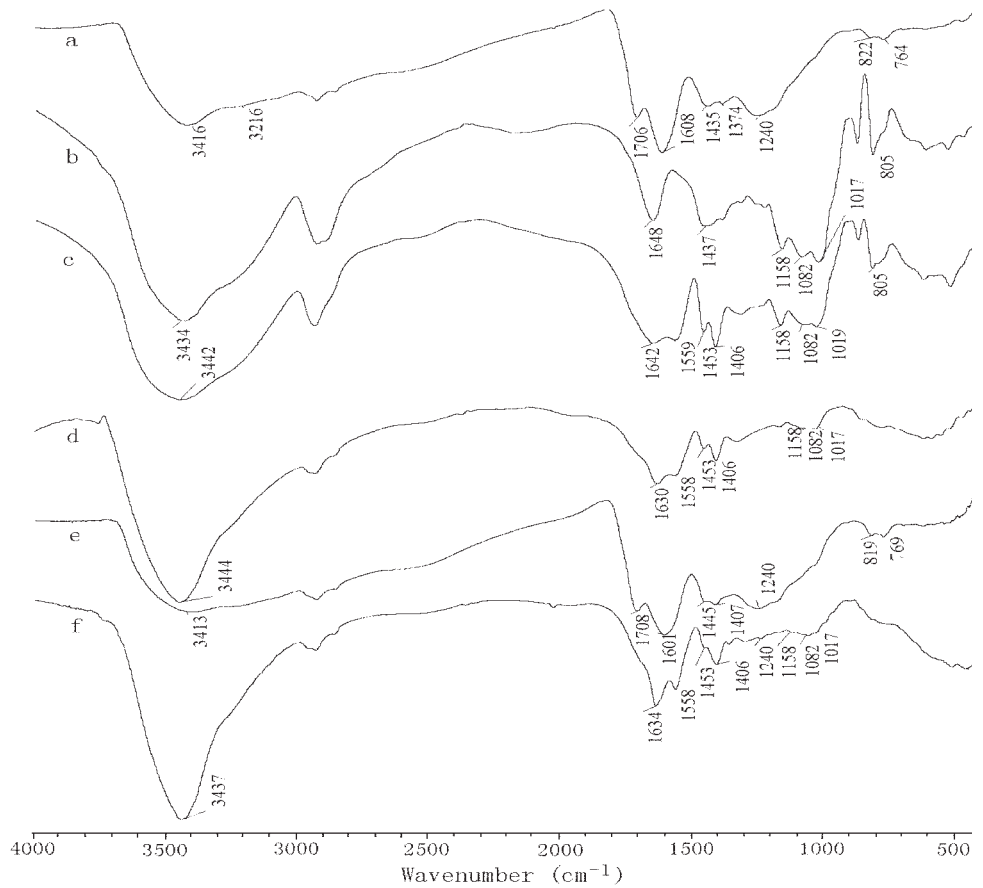

Figure 1 FTIR spectra of (a) SH, (b) GG, (c) a mixture of GG and PNaA, (d) GG-*g*-PNaA, (e) a mixture of GG-*g*-PNaA and SH, and (f) GG-*g*-PNaA/SH (15 wt %).

GG-*g*-PNaA, a physical mixture of GG-*g*-PNaA and SH (weight ratio of GG-*g*-PNaA to SH = 5.6), and GG-*g*-PNaA/SH (15 wt %) are shown in Figure 1. As can be seen from Figure 1(b), the absorption bands of GG at 1017, 1082, and 1158 cm^{-1}, ascribed to the stretching of C—O in the rings, the C—OH stretching vibration, and the stretching vibration of C—O—C in the rings, appear in the spectrum of the physical mixture of GG and PNaA [Fig. 1(c)] with a considerable peak intensity, but these characteristic bands of GG have almost disappeared in the spectra of GG-*g*-PNaA [Fig. 1(d)] and GG-*g*-PNaA/SH [Fig. 1(f)]; this implies the occurrence of a chemical reaction between GG and PNaA. In addition, the absorption bands of GG at 1648 and 1437 cm^{-1} (—OH bending) have disappeared, and the new absorption bands at 1630 (the C=O stretching of —COOH groups), 1558 (asymmetric stretching of —COO$^-$ groups), and 1452 and 1405 cm^{-1} (symmetric stretching of —COO$^-$ groups) appear in the FTIR spectra of GG-*g*-PNaA and GG-*g*-PNaA/SH. This information indicates that the PNaA chains have been grafted onto the macromolecular chains of GG. Furthermore, a comparison with the FTIR spectrum of SH [Fig. 1(a)] shows that the absorption bands of SH at 3216 (N—H stretching), 1706 (C=O stretching), 1608 (—COO$^-$ asymmetric stretching), and 1374 cm^{-1} (C—OH bending) are absent in the spectrum of GG-*g*-PNaA/SH, and new bands at 1632 and 1558 cm^{-1} can be observed in the spectrum of GG-*g*-PNaA/SH. The band of SH at 1240 cm^{-1} (phenolic C—O stretching) has almost disappeared in the spectrum of GG-*g*-PNaA/SH [Fig. 1(f)], and the characteristic absorption bands of SH at 822 and 764 cm^{-1} disappear after the polymerization reaction. However, the characteristic absorption bands of SH at 1608, 1240, 822, and 764 cm^{-1} can be clearly observed in the spectrum of the physical mixture of GG-*g*-PNaA and SH [Fig. 1(e)]. Generally, changes in the characteristic peaks of GG and SH before and after the reaction provide direct evidence that a graft copolymerization reaction has taken place between GG, neutralized AA, and SH, and similar results have been reported in previous studies on superabsorbents containing SH.[23]

Morphological analyses

The effect of introducing SH on the surface morphologies of superabsorbents was observed with

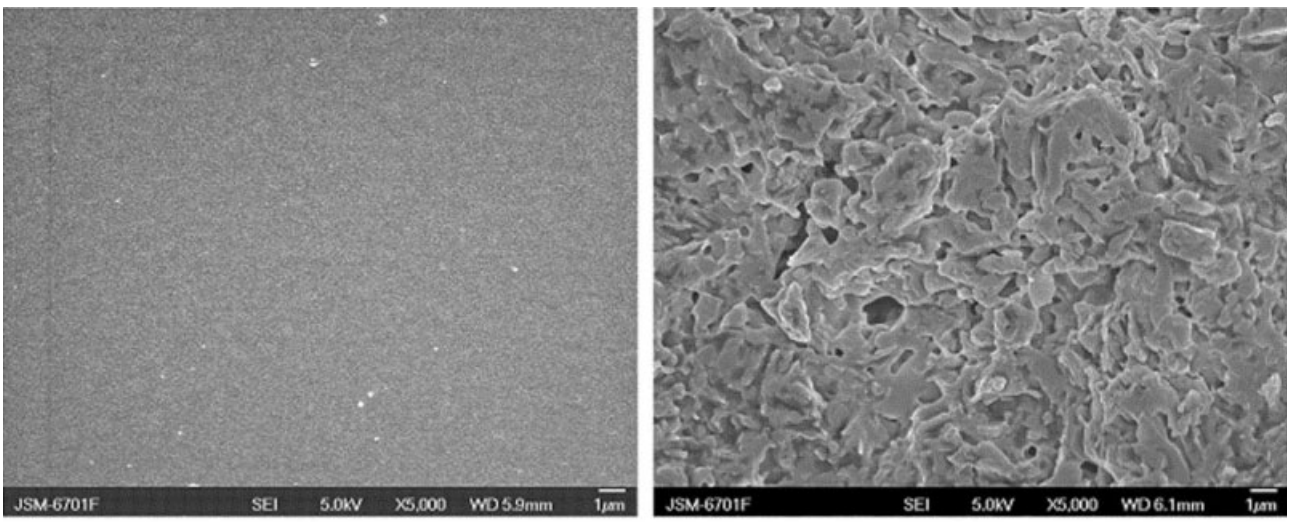

Figure 2 Scanning electron micrographs of (a) GG-*g*-PNaA and (b) GG-*g*-PNaA/SH (15 wt %).

scanning electron microscopy and is shown in Figure 2. GG-*g*-PNaA shows a dense, tight, and smooth surface without any pores [Fig. 2(a)], whereas GG-*g*-PNaA/SH exhibits a loose, coarse, and porous surface [Fig. 2(b)]. The coarse and porous surface causes an increase in the surface area of the superabsorbent, which allows the aqueous fluid to diffuse into the polymeric network and provides the final superabsorbent with high water absorbency.[24,25] This observation also directly reveals that SH is almost embedded within the GG-*g*-PNaA polymeric network and equally dispersed in the polymer matrix without aggregation; this facilitates the formation of a homogeneous composition for the resulting superabsorbent.

Thermal stability

The effect of introduced SH on the thermal stability of the resulting superabsorbent was investigated with thermogravimetric analyses and is depicted in Figure 3. Both GG-*g*-PNaA and GG-*g*-PNaA/SH (15 wt %) show three-stage thermal decomposition, and the weight-loss rate of GG-*g*-PNaA is obviously faster than that of GG-*g*-PNaA/SH. In the initial stage, a weight loss of about 19.1% between 25 and 340°C for GG-*g*-PNaA indicates the loss of moisture absorbed in it, the dehydration of saccharide rings, the breaking of C—O—C bonds in the chain of GG, and the elimination of the water molecule from the two neighboring carboxylic groups of the grafted chains due to the formation of anhydride.[26] However, this process is delayed and shows a weight loss of 17.8% in the temperature range of 259–376°C for GG-*g*-PNaA/SH. The successive weight losses of about 13.8% from 340 to 430°C for GG-*g*-PNaA and of about 8.9% in the range of 376–433°C for GG-*g*-PNaA/SH can be attributed to the destruction of carboxylic groups and CO_2 evolution as well as main-chain scission.[27] The weight losses of about 21.6% from 430 to 494°C for GG-*g*-PNaA and about 17.5% from 433 to 513°C for GG-*g*-PNaA/SH are due to the breakage of PNaA chains and the destruction of the crosslinked network structure. In comparison with GG-*g*-PNaA, GG-*g*-PNaA/SH shows lower total weight loss, and this indicates that the introduction of SH into the GG-*g*-PNaA polymeric network enhances the thermal stability of the superabsorbent because of the formation of chemical bonds between SH and the GG-*g*-PNaA polymeric network.

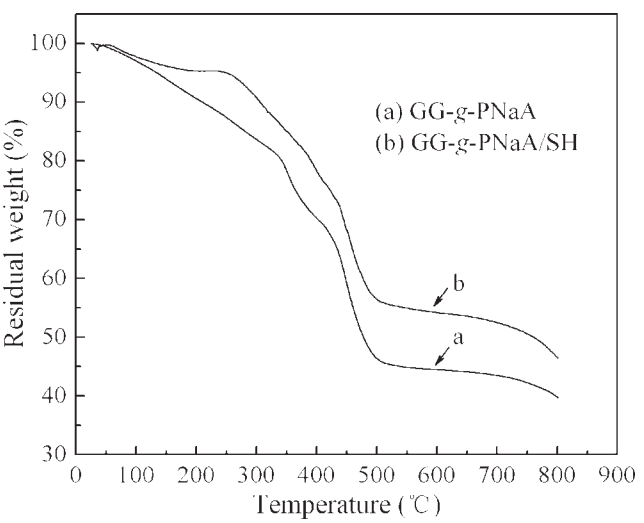

Figure 3 Thermogravimetric analysis curves of (a) GG-*g*-PNaA and (b) GG-*g*-PNaA/SH (15 wt %).

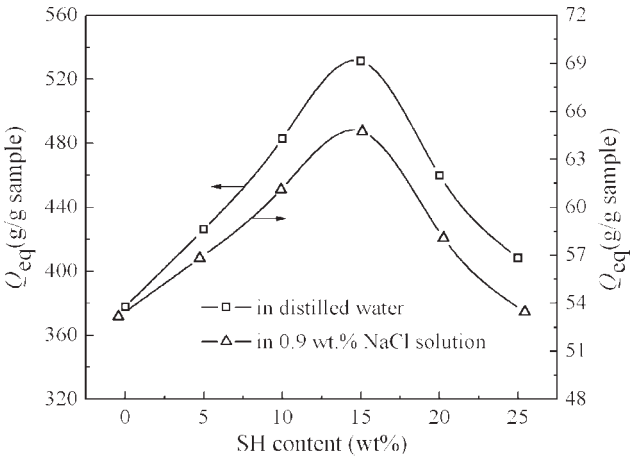

Figure 4 Effect of the SH content on the water absorbency.

Effect of the SH content on the water absorbency

The effect of the SH content on water absorbency is shown in Figure 4. The water absorbency of the superabsorbent remarkably increases with the SH content increasing to 15 wt % and then decreases, and the water absorbency of the superabsorbent containing 15 wt % SH is 41% higher than that of the sample without SH. The improvement of the water absorbency can be attributed to the following. First, SH contains plentiful hydrophilic groups such as —COO^-, —OH, and —NH_2 [Scheme 1(b)], which can participate in the polymerization reaction and the construction of a three-dimensional network. As a result, the introduction of moderate amounts of SH into the GG-*g*-PNaA network improves the network structure and enhances the water absorbency. Second, the incorporation of SH results in an increase in the amount of phenolic hydroxyl and acylamino groups in the superabsorbent. Because the collaborative absorbent effect of —$CONH_2$, —OH, and —COOH or —COONa groups are superior to that of single —COOH or —COONa groups,[28] the water absorbency of the superabsorbent increases. However, a further increase in the SH content from 15 to 25 wt % leads to a reduction of the water absorbency. As is known, the number of hydrophilic groups on the polymeric backbone decreases with increasing SH content; this causes a reduction of the osmotic pressure difference between the polymeric network and the external solution and follows the reduction of the water absorbency. Also, excessive SH powder can act as padding in the polymeric network.[29] In addition, the water absorbency of the superabsorbent incorporating 25 wt % SH is still 8% higher than that of the sample without SH; this is favorable for reducing the production cost.

Effects of the MBA concentration

As can be seen in Figure 5, the MBA concentration has remarkable effects on the water absorbency of the superabsorbent. The water absorbency abruptly decreases with the MBA concentration increasing from 1.274 to 6.793 mmol/L. Although a crosslinker is essential to the construction of a three-dimensional hydrophilic network, a high crosslinker concentration may result in the generation of more crosslink points and an increase in the crosslinking density and directly lead to a reduction of the water absorbency. However, when the MBA concentration is lower than 1.274 mmol/L, SH cannot crosslink effectively with the polymeric network, and the water-holding network space cannot be formed adequately. Under this condition, the water absorbency of the superabsorbent is also low. The relationship between the equilibrium water absorbency and the MBA concentration follows the relation shown in eq. (6):[30]

$$Q_{eq} = kC_{MBA}^{(-n)} \tag{6}$$

where C_{MBA} is the concentration of MBA and k and n are constants for an individual superabsorbent that can be obtained from a curve fitted with eq. (6). In this series, the effect of the MBA concentration on the water absorbency follows the relation $Q_{eq} = 73.81C_{MBA}^{(-0.2724)}$ in distilled water and $Q_{eq} = 13.51C_{MBA}^{(-0.2312)}$ in a 0.9 wt % NaCl solution.

Effect of the SH content on the swelling kinetics

It is well known that the swelling kinetics of a superabsorbent material are significantly influenced by various factors such as the composition of the superabsorbent, the particle size, and the surface

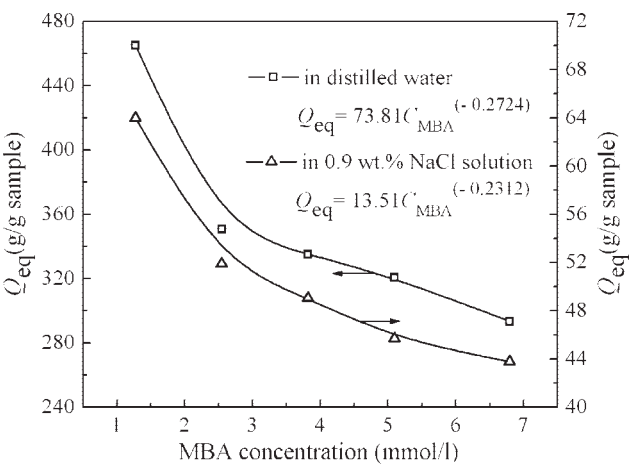

Figure 5 Effect of the MBA concentration on the water absorbency.

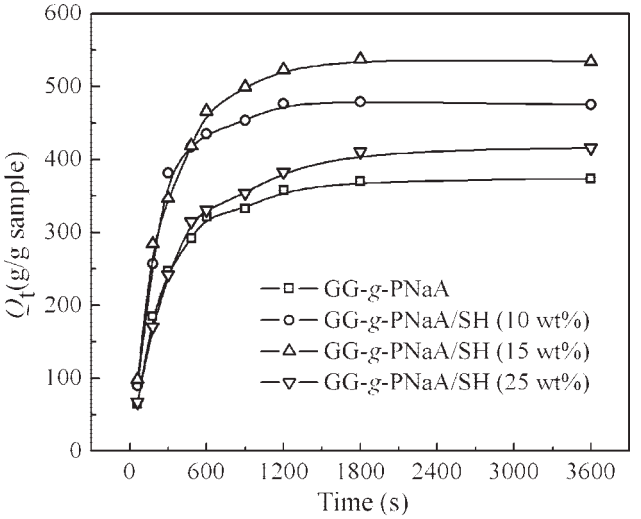

Figure 6 Swelling kinetics of superabsorbents containing various amounts of SH in distilled water. Q_t denotes the water absorbency (g/g of sample) of superabsorbents at the time t (s).

area.[31] Thus, the incorporation of various amounts of SH certainly affects the swelling kinetics of the resulting superabsorbent. The effects of the SH content on the swelling kinetics of the superabsorbents are shown in Figure 6 and can be expressed by the Voigt-based viscoelastic model:[32,33]

$$Q_t = p(1 - e^{-t/r}) \tag{7}$$

where Q_t is the water absorbency at time t (g/g of sample), p is the power parameter denoting the theoretical equilibrium water absorbency (g/g of sample), t is the time for Q_t (min), and r is the rate parameter for Q_t denoting the time required to reach 63% of the equilibrium water absorbency (min). The p and r values were obtained through the fitting of experimental data to eq. (7) and are listed in Table I. Because r is a measure of resistance to water permeation, a lower r value will reflect a higher swelling rate.[34] Thus, it can be concluded from the r values that the swelling rates for the samples follow this order: GG-*g*-PNaA/SH (10 wt %) > GG-*g*-PNaA/SH (15 wt %) > GG-*g*-PNaA > GG-*g*-PNaA/SH (25 wt %). As described by Lee and Wu,[35] the initial swelling progress is due primarily to the penetration of water into the polymeric network through capillarity and diffusion. The incorporation of SH can improve the surface structure and increase the surface area of the resulting superabsorbents [Fig. 2(b)]; this make water more easily diffuse into the polymeric network and leads to the increase in the swelling rate. However, when the content of SH exceeds 15 wt %, the ratio of hydrophilic groups (e.g., —COOH and —COO^-) in the GG-*g*-PNaA/SH superabsorbent decreases with increasing SH content. The shrinkage of hydrophilic groups can reduce the affinity of the polymeric network with water and then decrease the rate of water penetration of the polymeric network. In addition, the value of p can be used to evaluate the water-absorption capability of the superabsorbent. According to the fitted p values (Table I), it can be concluded that the theoretical water absorbency of the superabsorbents is close to the experimental values. The swelling capability of the superabsorbents can be evaluated as follows: GG-*g*-PNaA/SH (15 wt %) > GG-*g*-PNaA/SH (10 wt %) > GG-*g*-PNaA/SH (25 wt %) > GG-*g*-PNaA. This suggests that the changes in the polymeric structure and surface area resulting from the introduction of SH can not only improve the swelling rate but also enhance the water absorbency.

TABLE I
Swelling Kinetic Parameters of Superabsorbents with Various SH Contents in Distilled Water

Sample	Q_{eq} (g/g of sample)[a]	p (g/g of sample)[b]	r (s)
GG-*g*-PNaA	378	363	275.62
GG-*g*-PNaA/SH (10 wt %)	483	475	221.02
GG-*g*-PNaA/SH (15 wt %)	532	529	273.58
GG-*g*-PNaA/SH (25 wt %)	408	404	337.31

[a] Experimental equilibrium water absorbency.
[b] Theoretical equilibrium water absorbency.

Effect of the saline solution

The effect of saline on the water absorbency of the superabsorbent is especially significant for its practical application as a water-manageable material. As can be seen in Figure 7, the water absorbency of the

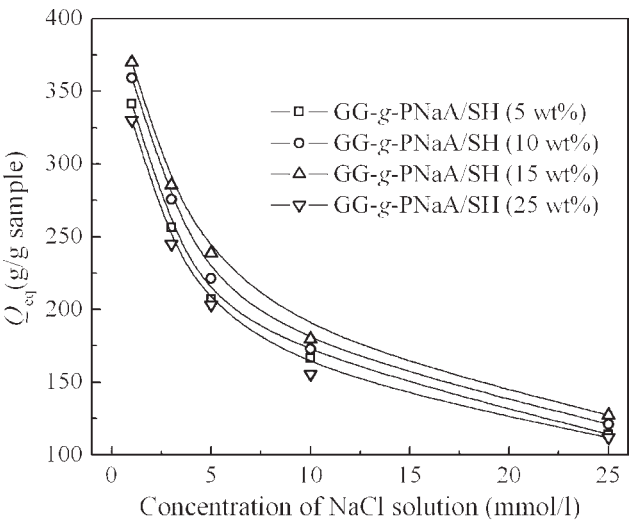

Figure 7 Effect of the concentration of the NaCl solution on the water absorbency.

TABLE II
Power-Law Constants for the Swelling Dependence of GG-*g*-PNaA/SH on the Concentration of the NaCl Solution

Sample	k	n	R^2
GG-*g*-PNaA/SH (5 wt %)	37.78	0.3212	0.9907
GG-*g*-PNaA/SH (10 wt %)	40.29	0.3199	0.9862
GG-*g*-PNaA/SH (15 wt %)	44.39	0.3106	0.9831
GG-*g*-PNaA/SH (25 wt %)	35.93	0.3234	0.9930

superabsorbent decreases with the concentration of the NaCl solution increasing. In saline media, the osmotic pressure difference between the gel network and external solution decreases, and the screening effect of the counterion (e.g., Na^+) with respect to negative —COO^- groups is enhanced when the concentration of the saline solution is increased. As a result, the driving force for water diffusing into the superabsorbent is weakened, and then the water absorbency decreases. The effect of the concentration of the saline solution on the water absorbency follows the relationship shown in eq. (8):[33]

$$Q_{eq} = kC_{saline}^{(-n)} \tag{8}$$

where C_{saline} is the concentration of the saline solution and k and n are power-law constants for an individual superabsorbent that can be obtained from the curve fitted with eq. (8). The calculated constants are listed in Table II. The exponent n decreases with the content of SH increasing from 5 to 15 wt % and then increases with a further increase in the SH content to 25 wt %. However, the constant k takes on an inverse tendency.

Effect of the pH value of the external solution

In practical applications, the sensitivity of an agricultural superabsorbent to the pHs of the external aqueous media or soil is not a negligible factor. In this section, the equilibrium water absorbency of GG-*g*-PNaA/SH is studied at various pHs ranging from 2 to 13 [Fig. 8(a)]. The superabsorbent can maintain high water absorbency over a wide pH range of 4–11. To investigate this behavior, the pH values of an external solution after swelling were determined, and the results are shown in Figure 8(b). When the pH is less than 4 or greater than 11, the pH of the external solution changes only a little after swelling, in contrast to the pH before swelling. However, the pH values greatly change because of the swelling of the superabsorbent [Fig. 8(b)] in the pH range of 4–11. As an anion-type superabsorbent, GG-*g*-PNaA/SH contains large amounts of —COOH and —COO^- groups; —COO^- groups can combine with H^+ of the external solution under an acidic condition, and —COOH groups can react with external OH^- to convert to —COO^- under a basic condition. As a result, the amount of H^+ and OH^- in the external solution may decrease in the pH range of 4–11 because of the buffer action of —COOH and —COO^- groups.[35] A similar result can be observed in chitosan-*g*-poly(acrylic acid)/organorectorite,[36] and this is very advantageous for the use of superabsorbents in various soils for agricultural and ecological projects. However, the buffer action disappears when the pH is less than 4 or greater than 11. In an acidic medium (pH < 4), increasing the pH of the external solution may enhance the ionized degree of hydrophilic groups, and this can induce an increase in the osmotic swelling pressure as well as the electrostatic repulsion among —COO^- groups.[37] Thus, the polymeric network more easily expands and holds more water. When the pH of the external solution exceeds 11, the increased ionic strength of the external solution causes the rapid reduction of the osmotic

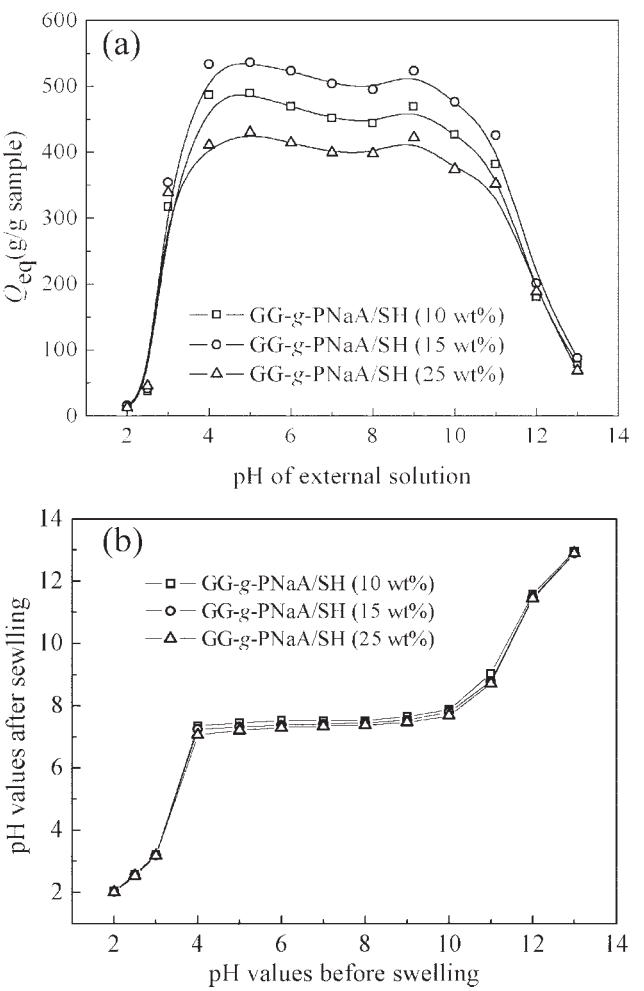

Figure 8 (a) Effect of the pH of the external solution on the water absorbency and (b) pH values of the external solution after swelling as a function of the pH values before swelling.

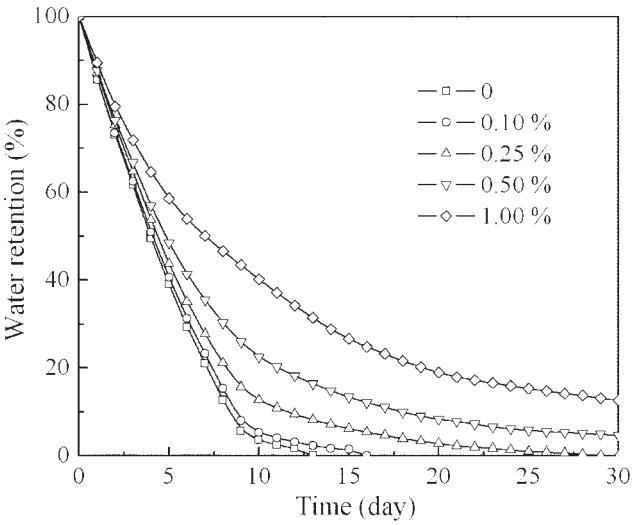

Figure 9 Practical water-retention curves of the GG-*g*-PNaA/SH (15 wt %) superabsorbent with various dosages in sandy soil.

swelling pressure and ultimately reduces the equilibrium swelling capacity of the superabsorbent.

Practical water-retention properties in sandy soil

The practical water retention in sandy soil of a superabsorbent as a water-manageable material is essential to its applications in agriculture and even in the recovery of desolate desert. As shown in Figure 9, the content of water remaining in sandy soil decreases with the time increasing, but the reduction rate is obviously different for sandy soil with and without the superabsorbent. The sandy soil mixed with the GG-*g*-PNaA/SH (15 wt %) superabsorbent exhibits a slower water-evaporation rate versus that without the superabsorbent. The sandy soil without the superabsorbent loses almost all of the absorbed water at 13 days, whereas the water-retention period of the sandy soil dosed with a 1 wt % concentration of the superabsorbent can be prolonged to 30 days, and 12.62% of the initial absorbed water can still remain after 30 days. As described previously, the use of GG-*g*-PNaA/SH in sandy soil obviously improves its water-holding capability. Therefore, the superabsorbent can be used as an effective water-saving material for agriculture and ecological recovery.

Slow-release properties

Curves of the slow release of SH from the GG-*g*-PNaA/SH superabsorbent in distilled water are shown in Figure 10, and this can be denoted as the carbon content in 5 mL of solution. The release rate is higher in the initial stages and then gradually slows after the initial release. The carbon contents reach 0.16, 0.24, and 0.28 g/5 mL on day 10 for the superabsorbents containing 10, 15, and 25 wt % SH, respectively. The carbon content increases with the increase in the SH content in the GG-*g*-PNaA/SH superabsorbents. The rapid release in this period can be mainly ascribed to the dissolution of SH on the surface of the superabsorbents as well as SH filled physically in the polymeric network. Ten days later, the release rate obviously decreases, and the carbon contents increase gradually to 0.22, 0.28, and 0.32 g/5 mL for the superabsorbents containing 10, 15, and 25 wt % SH, respectively, after 60 days. The slow release rate might be attributed to the release of SH bonded with the polymeric network, which needs more time to diffuse from the superabsorbent granule into the water. The release behavior of SH in the superabsorbents is similar to the behavior of other conventional slow-release fertilizers.[38] Thus, the superabsorbents possess a slow-release property and can be used as fertilizers.

Reswelling capability

The reusability of superabsorbent materials is also an important factor affecting their effective usage. As shown in Figure 11, the resulting dry superabsorbent still shows a better water-absorption capability after the swollen superabsorbent is thoroughly dewatered. Also, the superabsorbent can maintain 79.4 (10 wt % SH), 90.7 (15 wt % SH), and 85.2% (25 wt % SH) of the initial water absorbency after swelling three times. The water absorbency of the superabsorbent can also reach 50.1 (10 wt % SH), 52.9 (15 wt % SH), and 48.4% (25 wt % SH) of the initial water absorbency even after reswelling six times. These results indicate that the superabsorbent

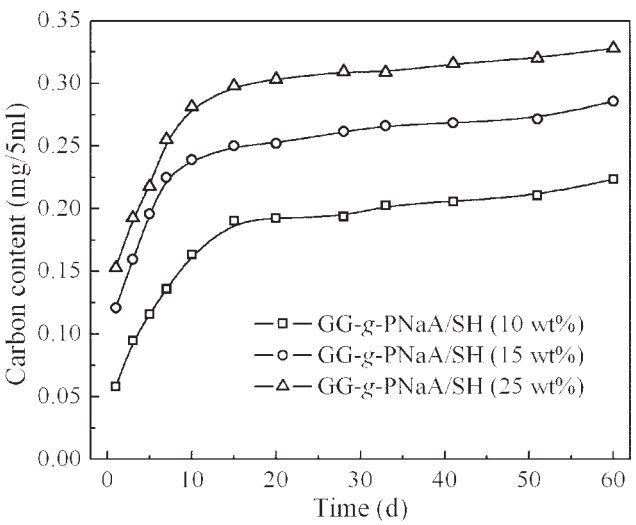

Figure 10 Slow-release curves of SH from GG-*g*-PNaA/SH in distilled water.

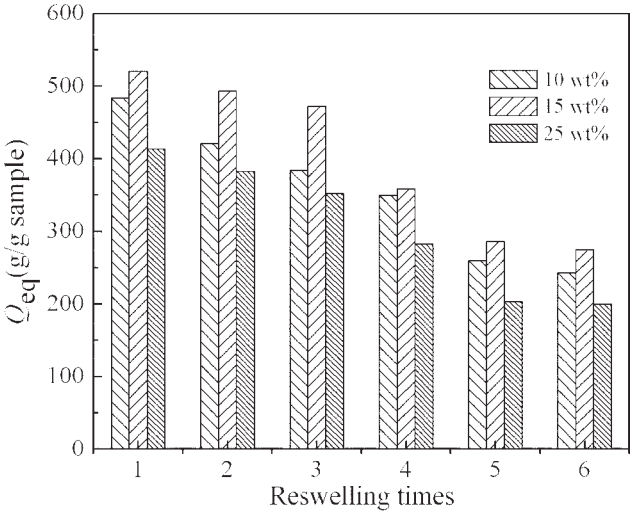

Figure 11 Water absorbency of the superabsorbents as a function of the reswelling times.

possesses a better reswelling capability, is reusable and recyclable, and can be used as a potential water-managing material.

CONCLUSIONS

As part of the effort to prepare a superabsorbent for agricultural and ecological projects, an environmentally friendly GG-*g*-PNaA/SH superabsorbent polymer with a slow-release fertilizer has been prepared by graft copolymerization between naturally renewable GG and partially neutralized AA with the participation of functional SH in an aqueous solution. Under optimal conditions, the best absorption of the superabsorbent is 532 g/g of sample in distilled water and 62 g/g of sample in a 0.9 wt % NaCl solution. SH can be used directly as a raw mineral without further treatment and can effectively participate in the polymerization reaction; therefore, the preparation procedure can be simplified greatly. Furthermore, superabsorbents based on natural resources and SH exhibit improved water-absorption and water-retention capabilities and swelling rates, pH-resistant properties, and reusability. The GG-*g*-PNaA/SH superabsorbent is a suitable candidate for applications in agriculture and ecological recovery.

References

1. Malowaniec, K. D. U.S. Pat. 6,414,216 B1 (2002).
2. Omidiana, H.; Roccaa, J. G.; Park, K. J Control Release 2005, 102, 3.
3. Guilherme, M. R.; Reis, A. V.; Paulino, A. T.; Fajardo, A. R.; Muniz, E. C.; Tambourgi, E. B. J Appl Polym Sci 2007, 105, 2903.
4. Wang, L.; Zhang, J. P.; Wang, A. Q. Colloids Surf A 2008, 322, 47.
5. Chen, P.; Zhang, W. A.; Luo, W.; Fang, Y. E. J Appl Polym Sci 2004, 93, 1748.
6. Raju, K. M.; Raju, M. P.; Mohan, Y. M. Polym Int 2003, 52, 768.
7. Chu, M.; Zhu, S. Q.; Li, H. M.; Huang, Z. B.; Li, S. Q. J Appl Polym Sci 2006, 102, 5137.
8. Kiatkamjornwong, S.; Mongkolsawat, K.; Sonsuk, M. Polymer 2002, 43, 3915.
9. Wu, L.; Liu, M. Z. Carbohydr Polym 2008, 72, 240.
10. Yoshimura, T.; Matsuo, K.; Fujioka, R. J Appl Polym Sci 2006, 99, 3251.
11. Lanthong, P.; Nuisin, R.; Kiatkamjornwong, S. Carbohydr Polym 2006, 66, 229.
12. Cao, Y. M.; Qing, X. S.; Sun, J. Eur Polym J 2002, 38, 1921.
13. Ibrahim, S. M.; El Salmawi, K. M.; Zahran, A. H. J Appl Polym Sci 2007, 104, 2003.
14. Suo, A. L.; Qian, J. M.; Yao, Y.; Zhang, W. G. J Appl Polym Sci 2007, 103, 1382.
15. Zhang, J. P.; Wang, L.; Wang, A. Q. Ind Eng Chem Res 2007, 46, 2497.
16. Mahdavinia, G. R.; Pourjavadi, A.; Hosseinzadeh, H.; Zohuriaan, M. J. Eur Polym J 2004, 40, 1399.
17. Pourjavadi, A.; Ghasemzadeh, H.; Soleyman, R. J Appl Polym Sci 2007, 105, 2631.
18. Pourjavadi, A.; Amini-Fazl, M. S.; Barzegar, S. J Appl Polym Sci 2008, 107, 2970.
19. Greenwald, H. L.; Luskin, L. K. S. In Handbook of Water Soluble Gums and Resins; Davidson, R. L., Ed.; McGraw-Hill: New York, 1980; p 19.
20. Li, A.; Zhang, J. P.; Wang, A. Q. J Appl Polym Sci 2007, 103, 37.
21. Zhang, J. P.; Li, A.; Wang, A. Q. React Funct Polym 2006, 66, 747.
22. Zheng, Y. A.; Gao, T. P.; Wang, A. Q. Ind Eng Chem Res 2008, 47, 1766.
23. Hua, S. B.; Wang, A. Q. Carbohydr Polym 2009, 75, 79.
24. Liu, P. S.; Li, L.; Zhou, N. L.; Zhang, J.; Wei, S. H.; Shen, J. J Appl Polym Sci 2007, 104, 2341.
25. Santiago, F.; Mucientes, A. E.; Osorio, M.; Rivera, C. Eur Polym J 2007, 43, 1.
26. Taunk, K.; Behari, K. J Appl Polym Sci 2000, 77, 39.
27. Huang, Y. H.; Lu, J.; Xiao, C. B. Polym Degrad Stab 2007, 92, 1072.
28. Wu, J. H.; Lin, J. M.; Li, G. Q.; Wei, C. R. Polym Int 2001, 50, 1050.
29. Lin, J. M.; Wu, J. H.; Yang, Z. F.; Pu, M. L. Macromol Rapid Commun 2001, 22, 422.
30. Flory, P. J. Principles of Polymer Chemistry; Cornell University Press: New York, 1953.
31. Buchanan, K. J.; Hird, B.; Letcher, T. M. Polym Bull 1986, 15, 325.
32. Omidian, H.; Hashemi, S. A.; Sammes, P. G.; Meldrum, I. G. Polymer 1998, 39, 6697.
33. Kabiri, K.; Omidian, H.; Hashemi, S. A.; Zohuriaan-Mehr, M. J Eur Polym J 2003, 39, 1341.
34. Pourjavadi, A.; Mahdavinia, G. R. Turk J Chem 2006, 30, 595.
35. Lee, W. F.; Wu, R. J. J Appl Polym Sci 1996, 62, 1099.
36. Liu, J. H.; Wang, A. Q. J Appl Polym Sci 2008, 110, 678.
37. Kiatkamjornwong, S.; Chomsaksakul, W.; Sonsuk, M. Radiat Phys Chem 2000, 59, 413.
38. Liu, M. Z.; Liang, R.; Zhan, F. L.; Liu, Z.; Niu, A. Z. Polym Adv Technol 2006, 17, 430.